

# Existence and stability of nonlinearly coupled electromagnetic and electrostatic relativistic wave solutions during laser-plasma-interaction

G. Lehmann, E.W. Laedke, K.H. Spatschek

*Institut für Theoretische Physik, Heinrich-Heine-Universität Düsseldorf*

*D-40225 Düsseldorf, Germany*

Based on a relativistic fluid-Maxwell model laser-induced plasma dynamics is investigated for relativistic periodic waves. Within a one-dimensional (1D) description the Akhiezer-Polovin model is applied to the existence and stability of periodic, nonlinearly coupled electromagnetic and electrostatic waves and the corresponding particle motion. Known existence criteria for periodic solutions are generalized. The corresponding stability behaviors are investigated by linear 1D integrators of the relativistic fluid-Maxwell model.

We use a one-dimensional fluid-Maxwell model to describe the plasma, i.e. variations of all quantities are only considered along the direction of propagation  $x$ . The ions form a fixed homogeneous background. Dimensionless quantities are used. Length  $x$ , time  $t$ , velocity  $\mathbf{v}$ , momentum  $\mathbf{p}$ , vector  $\mathbf{A}$  and scalar potential  $\phi$ , density  $n$  are normalized by  $c/\omega_{pe}$ ,  $\omega_{pe}^{-1}$ ,  $c$ ,  $m_e c$ ,  $m_e c/e$ ,  $m_e c^2/e$ , and  $n_0$  respectively. Here,  $\omega_{pe} = (n_0 e^2 / \epsilon_0 m_e)^{1/2}$  is the electron plasma frequency,  $m_e$  the electron rest mass,  $e$  the electron charge, and  $n_0$  the unperturbed electron density. Maxwell's equations will be expressed in the Coulomb gauge, which leads to  $\mathbf{A} \equiv \mathbf{A}_\perp$  as a result of the 1D model. A further consequence of the 1D geometry is that  $\mathbf{p}_\perp = \mathbf{A}_\perp$ . The hydrodynamic equations for the density  $n$ , the (parallel) momentum  $p$  of electrons, and the Maxwell equations for the vector and scalar potentials  $\mathbf{A}_\perp$  and  $\phi$  can be written in dimensionless form as

$$\begin{aligned} \frac{\partial^2 \mathbf{A}_\perp}{\partial x^2} - \frac{\partial^2 \mathbf{A}_\perp}{\partial t^2} &= \frac{n \mathbf{A}_\perp}{\gamma}, & \frac{\partial^2 \phi}{\partial x^2} &= n - 1, \\ \frac{\partial n}{\partial t} + \frac{\partial}{\partial x} \left( \frac{np}{\gamma} \right) &= 0, & \frac{\partial p}{\partial t} &= \frac{\partial}{\partial x} (\phi - \gamma), \end{aligned} \quad (1)$$

where  $\gamma = \sqrt{1 + |\mathbf{A}_\perp|^2 + p^2}$  is the relativistic factor.

We transform the system (1) to a frame of reference moving with the phase-velocity  $\beta$  of an electromagnetic wave. In this frame we are looking for solutions that do not depend explicitly on  $t$ , only on  $\xi = x - \beta t$ . For such stationary solutions it is possible to reduce the system (1) in the co-moving frame to equations for the potentials  $\phi$  and  $\mathbf{A}_\perp$ . All other quantities can be expressed as functions of the potentials. Considering a linearly polarized wave  $\mathbf{A}_\perp = a \hat{\mathbf{e}}_z$  (with  $|\mathbf{A}_\perp| = a_0$  and  $p = 0$  where  $\phi = 0$ ) the expression for the density  $n$ , parallel momentum  $p$ , and

the relativistic  $\gamma$  factor are

$$p = \frac{\beta\psi - R}{1 - \beta^2}, \quad n = \beta \frac{\psi - \beta R}{R(1 - \beta^2)}, \quad \gamma = \frac{\psi - \beta R}{1 - \beta^2}, \quad (2)$$

where  $\psi = \phi + \sqrt{1 + a_0^2}$ ,  $R = \sqrt{\psi^2 - (1 - \beta^2)(1 + a^2)}$ . The coupled equations for the potentials will be rewritten in terms of  $X = a(\beta^2 - 1)^{1/2}$ ,  $Z = -\phi - (1 + a_0^2)^{1/2}$ , and  $\zeta = \xi(\beta^2 - 1)^{-1/2}$  yields the nonlinear coupled oscillators  $X$  and  $Z$  of the form

$$\ddot{X} + \frac{\beta X}{\sqrt{\beta^2 - 1 + X^2 + Z^2}} = 0, \quad \ddot{Z} + \frac{\beta Z}{\sqrt{\beta^2 - 1 + X^2 + Z^2}} + 1 = 0. \quad (3)$$

The dots denote derivatives with respect to  $\zeta$ . These oscillators can be derived from the Hamiltonian  $H = \frac{1}{2}(\dot{X}^2 + \dot{Z}^2) + \beta(\beta^2 - 1 + X^2 + Z^2)^{1/2} + Z$ . Equations (3) are equivalent to the equations derived by Akhiezer and Polovin [1] (Eqs. (16) therein).

The plasma motion (in  $x, y, z$  direction) associated with the coupled transverse-longitudinal oscillators can be calculated from solutions  $X$  and  $Z$  as

$$\frac{dx(\zeta)}{d\zeta} = -\frac{\beta Z + \sqrt{Z^2 + X^2 \beta^2 - 1}}{\sqrt{\beta^2 - 1}}, \quad \frac{dz(\zeta)}{d\zeta} = -\frac{X}{\sqrt{Z^2 + X^2 \beta^2 - 1}}. \quad (4)$$

Interpreting  $\zeta$  as the parameter for the curves  $x = x(\zeta)$  and  $z = z(\zeta)$  we can draw the path  $x = x(z)$ .

Akhiezer and Polovin [1], Kaw and Dawson [2], and Chian and Clemmow [3] were amongst the first to discuss exact periodic solutions. Linearly polarized solutions with small longitudinal momenta with frequency  $2\omega$  and transversal momenta of frequency  $\omega$  were found. The resulting motion is an average drift of the plasma in propagation direction of the wave and an superposed motion in the average drift frame. The motion within the average drift frame resembles an eight-like trajectory in the plane spanned by propagation and polarization direction.

Another class of possible solutions are circular motions, when transversal and longitudinal momenta are of the same order. This was noted by Akhiezer and Polovin [1], and worked out in more detail, for example, by Pesch and Kull [4].

## Overview over the complete class of stationary wave solutions

In order to investigate whether additional periodic solutions exist, we use the oscillator formulation (3) [7]. We calculate trajectories for the  $X$  and  $Z$  oscillators in four-dimensional phase space and render Poincaré section plots. Periodic solutions are identified by fix-points or island-chains within the plots. The projections are done by using one of the oscillators as a clock, while plotting the coordinates of the other one. From the trajectories of  $X$  and  $Z$  we calculate the plasma

motion in the average drift frame for periodic solutions. Figure 1 shows Poincaré section plots for  $\beta = 2.5$  and  $H = 53.4$ . Plotted is  $X$  versus  $\dot{X}$  every time that the  $Z$  oscillator has a minimum. We marked five sets of points which correspond to periodic trajectories. The point labeled  $e$  represents a purely longitudinal wave. The fix points  $a$  and  $c$  represent the figure-eight and circular motion, respectively. The hyperbolic fix-point  $b$  represents a deformed figure-eight like solution, where one loop of the eight is smaller than the other one. The island-chain labeled  $d$  represents a higher-order amplitude modulated solution. Figure 2 shows the according plasma motion in the average drift frame for the labeled points from Fig. 1.

The structure of the Poincaré section plots varies with the values  $H$  and  $\beta$ . Let us focus on the influence of  $\beta$  here, keeping  $H = 53$  fixed. The only solution that exists for every  $\beta$ , i.e. every plasma density below the critical density, is the figure-eight solution. Beginning with  $\beta = 1$  we observe that at  $\beta \approx 2.3$  a new fix-point appears. This is the fix-point of the circular motion. Between  $\beta \approx 2.3$  and  $\beta \approx 2.6$  a hyperbolic fix-point exists that is related to the deformed figure-eight motion. Amplitude modulated solutions exist only up to a certain velocity (about  $\beta \approx 2.6$ ), too. The simultaneous existence of circular, figure-eight and deformed figure-eight like trajectories at given  $H$  and fixed  $\beta$  has not been clearly stated in literature so far.

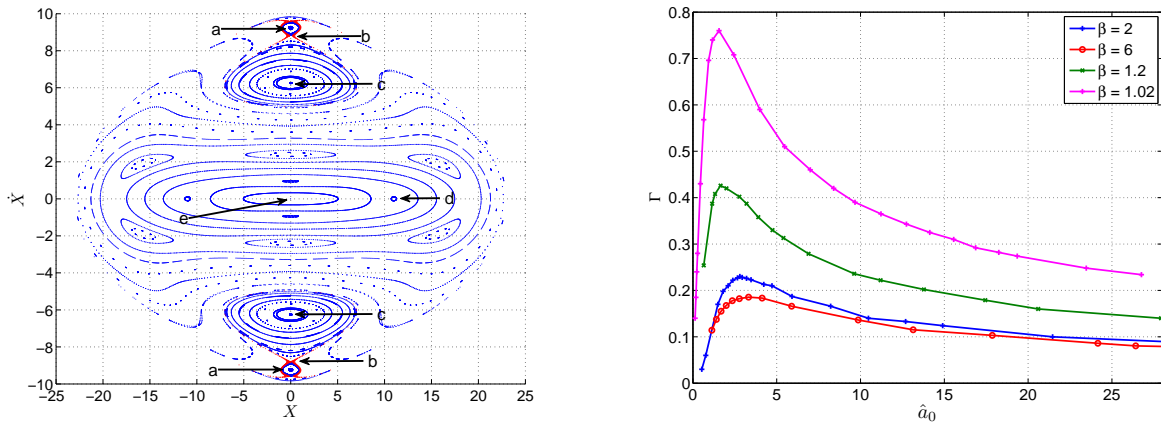


Figure 1: Left: Poincaré surface plot of  $X$  vs  $\dot{X}$  (for  $Z = Z_{min}$ ) for  $\beta = 2.5$  and  $H = 53.4$ . Labeled a to e are fix-points and island-chains that correspond to periodic solutions. The plasma motion for the labeled trajectories is shown in Fig. 2. Right: Growth rate  $\Gamma$  versus the maximum amplitude  $\hat{a}_0$  of the unperturbed figure-eight solution (labeled a on the right side) for  $\beta = 6$  (red line),  $\beta = 2$  (blue line),  $\beta = 1.2$  (green line) and  $\beta = 1.02$  (magenta line), respectively.

## Results on linear stability

The periodic solutions to Eqs. (3) are time-independent in the frame of reference moving with the phase-velocity  $\beta$ . Within this frame we carry out a stability analysis, investigating the influence of time-dependent perturbations. We study the effects that localized perturbations

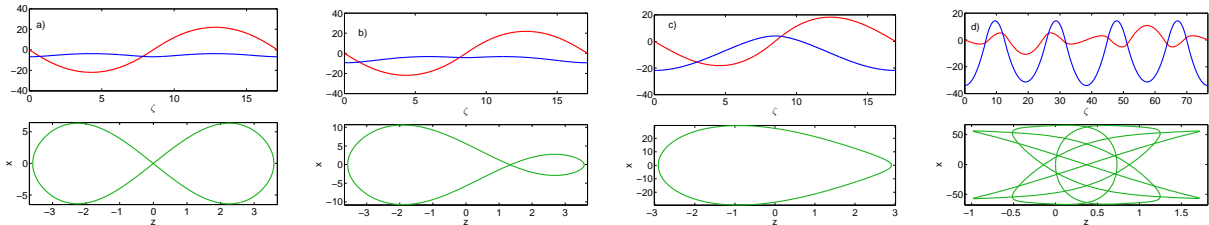


Figure 2: Oscillators  $X$  (red line) and  $Z$  (blue line) and corresponding plasma motion in the average drift frame (lower row, green line) for periodic solutions with  $\beta = 2.5$  and  $H = 53.4$ . From left to right: (a) figure eight, (b) deformed figure eight, (c) circular, and (d) higher order amplitude modulated solution.

have on the dynamics of the periodic solutions. The introduced initial perturbations are time-dependent, localized and have a non-zero energy. Perturbations of all quantities of the state (i.e.  $a$ ,  $p$ ,  $\phi$ ) are considered. Our numerical method allows us to calculate the most unstable mode and its growth rate  $\Gamma$ , for details see [5]. The results from our simulations of the linearized 1D Maxwell-fluid model show that all considered periodic wave solutions are unstable. We exemplify this for the figure-eight motion in Fig. 1. The growth rate  $\Gamma$  depends on the phase-velocity and the maximum amplitude of the solution. Typical growth rates are of the order of  $\Gamma = 0.1$  to  $\Gamma = 0.8$ . The typical time scale for a 1% perturbation with the fastest growing mode is of the order of a few tens of  $1/\omega_{pe}$ . Besides waves the model (1) also has pulsed solutions in the form of relativistic solitons. Our stability analysis for relativistic solitons shows that not all solitons, different from the nonlinear waves, are unstable in 1D geometry [5]. A comparison of growth rates for unstable solitons and nonlinear waves indicates that the growth rates for waves are about one order of magnitude larger [5, 6, 7]. Localization plays an important role for the scattering mechanism involved.

This work has been done under the auspices of the Sonderforschungsbereich TR-18.

## References

- [1] A. I. Akhiezer and R. V. Polovin. *Sov. Phys. JETP*, 3, 696 (1956).
- [2] P. Kaw and J. Dawson. *Phys. Fluids*, 13, 472 (1970).
- [3] A. C.-L. Chian and P. C. Clemmow. *J. Plasma Phys.*, 14, 505 (1975).
- [4] T. C. Pesch and H.-J. Kull. *Phys. Plasmas*, 14, 083103 (2007).
- [5] G. Lehmann, E. W. Laedke, and K. H. Spatschek. *Phys. Plasmas*, 13, 092302 (2006).
- [6] G. Lehmann, E. W. Laedke, and K. H. Spatschek. *Phys. Plasmas*, 15, 072307 (2008).
- [7] G. Lehmann and K. H. Spatschek. *Phys. Plasmas*, 17, in press, (2010).